CellPress

Trends in Biotechnology

Review

Nondestructive testing of native and tissue-engineered medical products: adding numbers to pictures

Nathan J. Castro [1], Greta Babakhanova [2], Jerry Hu [1], and K.A. Athanasiou [1,3,*]

Traditional destructive tests are used for quality assurance and control within manufacturing workflows. Their applicability to biomanufacturing is limited due to inherent constraints of the biomanufacturing process. To address this, photo- and acoustic-based nondestructive testing has risen in prominence to interrogate not only structure and function, but also to integrate quantitative measurements of biochemical composition to cross-correlate structural, compositional, and functional variances. We survey relevant literature related to single-mode and multimodal nondestructive testing of soft tissues, which adds numbers (quantitative measurements) to pictures (qualitative data). Native and tissue-engineered articular cartilage is highlighted because active biomanufacturing processes are being developed. Included are recent efforts and prominent trends focused on technologies for clinical and in-process biomanufacturing applications.

Highlights

Optics-based nondestructive techniques have shown to produce corroborative and congruent results to traditional tests.

Rapid, label-free, and quantitative spectroscopy can elucidate critical quality attributes when coupled to optical imaging and elastography for functional TEMPs.

Multimodal nondestructive tools can be facilitated by miniaturizing the form factor of probes leading to holistic assessment of tissues and TEMPs.

Fiber-coupled tools may be more amenable to coupling with other technologies as well as deployable aseptically for in-process and automated assessment of TEMPs while providing real-time feedback and quality control/assurance in scalable bioprocesses.

There is an outstanding need for standards development that will enable the translation, increase safety and reliability, improve in-process efficiency, and decrease the overall costs of TEMPs biomanufacturing.

Nondestructive testing of soft tissues

Nondestructive (see Glossary) qualitative and quantitative assessment of native and tissue-engineered soft tissues is a research area with great clinical and industrial potential. Specific to the biomanufacturing of **tissue-engineered medical products** (TEMPs), a core challenge of the field is in understanding and assessing the critical quality attributes of engineered tissues and correlating the critical process parameters and material attributes that greatly affect the intended clinical function [1]. Therefore, there is a growing need to develop nondestructive and noninvasive quantitative tools and methods to verify and to validate the critical biochemical components of TEMPs produced from a biological source, monitor extracellular matrix (ECM) development and composition, and correlate these critical components to tissue function (continuously and at predefined timepoints) [1].

For example, when developing TEMPs for **articular cartilage** (AC), the mechanical properties (function) of native tissue are used to qualify the robustness and project the long-term efficacy of developing and clinically used products [2]. One method of tissue engineering AC is using the self-assembling process, where mature chondrocytes are harvested, dedifferentiated, and subsequently redifferentiated *in vitro* to produce a more hyaline-like AC [3–5]. Tissue engineering is inherently time-, resource-, and cost-intensive, and the destructive testing used to verify and validate tissue-engineered AC can be inappropriate or impractical for scale-up and biomanufacturing. Therefore, nondestructive methods to assess the evolution of mechanical properties and correlate them back to structure and composition are needed to further the clinical translation of TEMPs.

The structure and composition of tissues has been independently evaluated by linear and nonlinear optics-based imaging techniques (e.g., **second-harmonic generation** (SHG) [6–9],

[1]Department of Biomedical Engineering, University of California Irvine, Irvine, CA 92617, USA
[2]Biosystems and Biomaterials Division, National Institute of Standards and Technology, Gaithersburg, MD, 20899, USA
[3]https://sites.uci.edu/deltai/

*Correspondence: athens@uci.edu (K.A. Athanasiou).

optical coherence tomography (OCT) [10–12], fluorescence microscopy [13–15], as well as vibrational spectroscopy [16–18], but each only tells part of the story. Even though nondestructive techniques for measuring tissue mechanical properties exist, few have been coupled with other nondestructive techniques to understand the structure–function correlates that critically affect the functionality of biomanufactured TEMPs.

One method that has shown potential to address the unmet need of correlating cartilage function to structural and compositional changes in a nondestructive manner is elastography. Elastography is an imaging technique used to interrogate the bulk mechanical properties of soft matter/tissues [19]. Researchers have also focused on coupling various nondestructive technologies [e.g., **optical coherence elastography** (OCE), **acoustic radiation force** (ARF)] to better understand the relationship between biochemical composition and mechanics to pathophysiology. Continuing development in miniaturization/downsizing the form factor of probes as well as retrofitting existing tooling has led to new single-/multimodal devices for minimally invasive assessment of tissues which may also prove suitable for **in-process testing** of TEMPs such as tissue-engineered AC in scalable bioprocesses. Therefore, in this perspective, we will look at single-/multimodal nondestructive testing of AC as an exemplary illustration of how such tests are generating correlative structure–function relationships, which can inform not only the diagnosis of cartilage pathologies but also methods to validate TEMPs.

Articular cartilage: structure, composition, and function

AC is the thin layer of hydrated soft connective tissue that covers the articulating surfaces of long and sesamoid bones within diarthrodial joints [20]. It protects bones from wear by providing lubrication, load distribution, and protection against shear stress during joint movement. Its deformability, which allows it to displace under dynamic compressive loading, is essential in reducing stress to the underlying bone [21] and is a direct function of the interplay between its primary structural and biochemical components as shown in Figure 1A.

Traditional assays including histological staining for tissue structure (hematoxylin and eosin) and collagen organization (picrosirius red), as well as colorimetric and fluorometric biochemical assays for components such as sulfated glycosaminoglycans (Alcian blue or Safranin O), cell density (PicoGreen), and collagen type (ELISAs) have been used to assess cartilage tissue properties. The primary drawback of these assays is their destructive nature that limits analyses to temporal snapshots of disease or state of maturation as opposed to longitudinal tracking of progression or ECM development. In addition, these assays can also require long digestion times or techniques that are prone to human error (e.g., manually taking histological sections). The drawbacks of traditional, destructive assays may be readily addressed through the adoption of validated and verified nondestructive tests. For detailed information of ACs' biochemical makeup, mechanics, and zonal distribution please see [22].

Nondestructive testing of AC

Nondestructive methods enable longitudinal tracking of samples, whereas the major limitation of destructive assays is that they only give snapshots of information about the state of the sample. In addition, nondestructive tests have been shown to produce analogous results to destructive assays for structure, composition, and function by probing some of the inherent properties of AC (Table 1). The measurands of AC listed in Table 1 are not exhaustive but serve to illustrate quantifiable attributes of AC which may serve as critical quality attributes within an application for regulatory approval.

Specifically, inherent tissue properties include optical properties for structural imaging (Figure 1B), molecular vibrations of constituent biomolecules (Figure 1C) for biochemical characterization, and

Glossary

Acoustic radiation force: nonlinear acoustic phenomenon that manifests itself as a nonzero force exerted by acoustic fields on particles.
Articular cartilage: smooth, white tissue that covers the ends of bones where they come together to form joints.
Birefringence (Δn): measure of optical anisotropy. It is defined as the maximum algebraic difference between two refractive indices measured in two perpendicular directions.
Brillouin microscopy: an empirical spectroscopy technique that uses the inelastic scattering of light when it encounters acoustic phonons in a crystal (Brillouin scattering). The technique allows for the determination of elastic moduli of materials.
Digital densitometry: an imaging-based method used to quantitatively measure the optical density of light-sensitive materials based on absorbance of specific wavelengths of energy.
Fluorescence lifetime imaging: technique by which fluorescence lifetime is imaged.
Fourier-transform infrared spectroscopy: technique used to obtain the absorption of infrared radiation by the sample material.
In-process testing: tests performed during a production process for the purpose of monitoring and, if necessary, to adjust the process to assure that the product conforms to its specifications.
Near-infrared spectroscopy: measurement of the wavelength and intensity of the absorption of near-infrared light by a sample. NIR light spans the 800– 500 nm (4000–12 500 cm^{-1}) range and is energetic enough to excite overtones and combinations of molecular vibrations to higher energy levels.
Nondestructive (test): method or technique used to detect and evaluate quality attributes in a material or system with no interaction between the sensor and the sample.
Optical coherence elastography: method to measure and display tissue elastic properties based on colocalization of doppler and optical coherence tomography imaging.
Optical coherence tomography: imaging technique characterized by high spatial resolution and noninvasive subsurface detection.
Optical coherence tomography quantitative microelastography: a tool consisting of an optical-fiber based

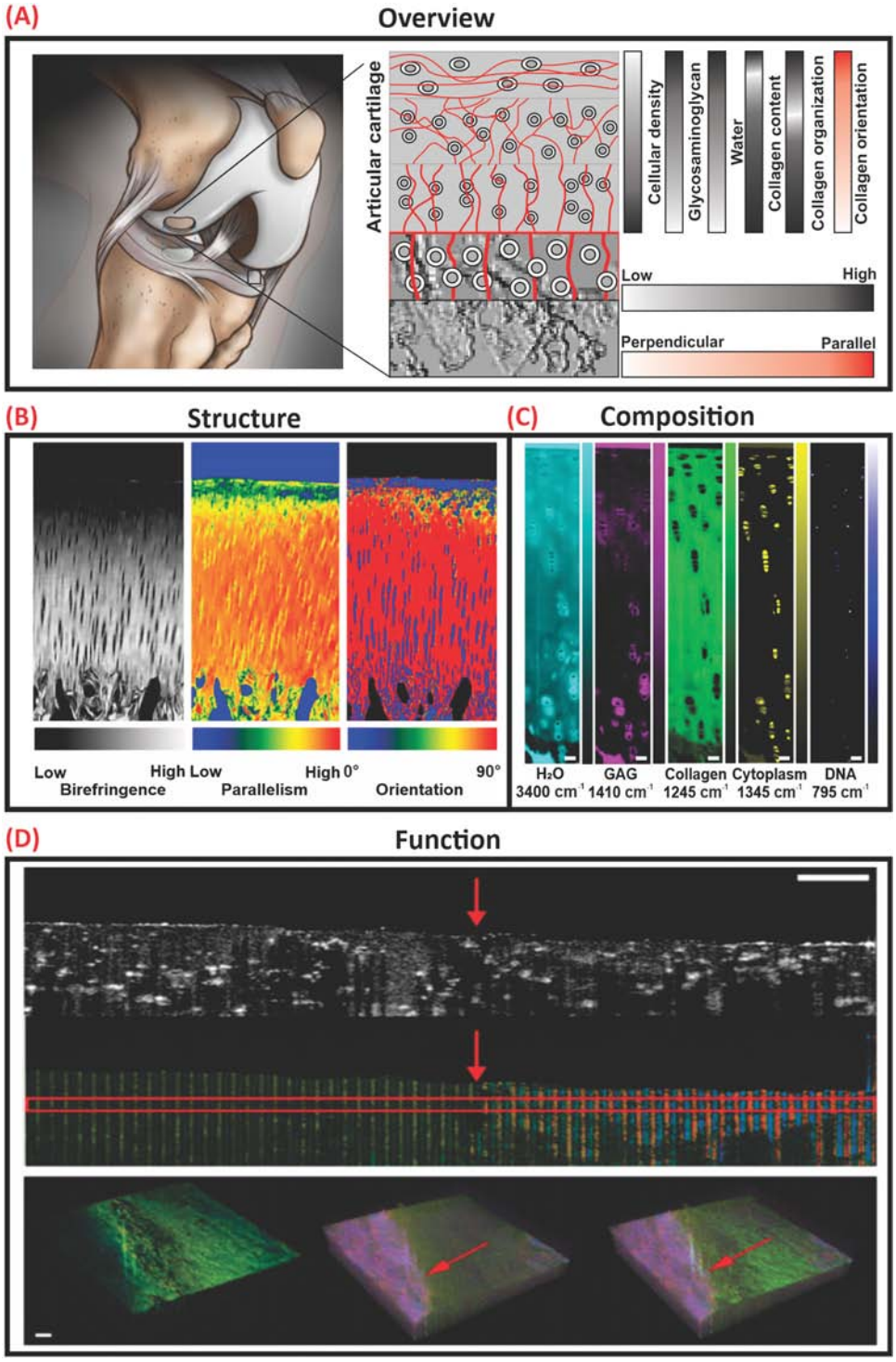

(See figure legend at the bottom of the next page.)

OCT system and, in most cases, a microelectromechanical ultrasound transducer for colocalized optical and doppler imaging of bulk material properties.

Osteoarthritis: a degenerative joint disease affecting articular cartilage and, in severe cases, the underlying bone.

Photoacoustic elastography: an elastographic technique wherein doppler images of photoacoustic generated soundwaves are captured and interrogated to assess bulk material properties.

Photoacoustic imaging: hybrid imaging technology based on the photoacoustic effect.

Raman spectroscopy: a vibrational spectroscopy technique based on inelastic light scattering (the Raman effect), which occurs when photons induce a change in the polarizability of molecules producing an optical fingerprint of the biomolecular constituents. The intensity of the measured Raman shifts is linearly proportional to the concentration of molecular constituents and can therefore be used to perform quantitative measurements.

Refractive index: ratio of the speed of radiation (light) in one medium to that in another medium.

Second-harmonic generation: the phenomenon that an input wave in a nonlinear material can generate a wave with twice the optical frequency.

Tissue-engineered medical product: a medical product that repairs, modifies or regenerates the recipient's cells, tissues, and organs or their structure and function, or both.

Tractography: a high-resolution visualization method of material characteristics and/or properties based on images acquired by various imaging modalities (e.g., OCT).

acoustic properties (Figure 1D) for bulk mechanical property evaluation. By coupling nondestructive techniques together within a multimodal platform, the critical quality attributes of functional TEMPs can be further understood. In addition, the nondestructive nature of these techniques allow for real-time feedback for in-process quality control.

Optical interrogation of AC structure

Optical material properties, including **refractive index** (RI) and **birefringence** (Δn) of biological tissues, have been of significant interest in a variety of disease diagnosis applications. Label-free quantitative polarized light microscopy yields the molecular orientation in biological samples and produces quantitative birefringence maps (Figure 2A) [26,39,40]. Both RI and Δn measurements have been used to assess AC microstructure as well as collagen degeneration; the latter through the disruption of the organized collagen network. Depth-dependent RI measurements show the RI distribution of normal AC as a regular ramp peaking in the middle-deep zone, while RI fluctuations associated with AC degeneration are attributed to the loss of proteoglycans [41]. Changes in Δn with respect to superficial AC has been postulated to be related to changes in the collagen network [42]. Birefringence can also be used to measure changes in cartilage thickness due to wear [43]. Therefore, RI and Δn are intrinsic optical properties of tissues which can be used to assess structural, and, to a certain extent, biochemical changes.

SHG is a polarization-sensitive, coherent, nonlinear optical process resulting from the interaction of two photons of the same frequency with non-centrosymmetric material (e.g., collagen and microtubules) generating a secondary photon with twice the energy of the incident photons. SHG provides endogenous contrast imaging of biological tissues and has a penetration depth of up to ~500 μm [44]. Limitations of the technique include its applicability to a small number of structural proteins and poor discrimination between biomolecules [45]; although it is possible to overcome the latter by incorporating polarization. Polarized SHG discriminates different molecular sources of SHG scattering (collagen I, collagen II, and myosin) based on their susceptibility value (Figure 2B) [46]. SHG microscopy provides intrinsic 3D sectioning capabilities with superior z-resolution enabling optical sectioning of biological samples with reduced out-of-plane phototoxicity allowing for the analysis of collagen orientation, distribution, and type (Figure 2B) [27,47]. Differentiating cartilage types in tissues is clinically relevant to identify disease progression such as **osteoarthritis** (OA); during which, the integrity and quality of hyaline cartilage (mainly composed of collagen II) degrades and is replaced with inferior fibrocartilage (mainly composed of collagen I) [46]. Therefore, cell-based TEMPs for cartilage repair would benefit from these capabilities as a means of monitoring ECM deposition and tissue maturation for quality assurance and control ensuring that the tissue-engineered AC is compositionally similar to native tissue.

Optoacoustic or **photoacoustic imaging** (PAI) provides structural information that has been used in clinical applications (Figure 2C). It achieves high-resolution imaging in deep biological tissues by combining high optical contrast and high ultrasound resolution in a single modality with micrometer-scale resolution and millimeter-scale imaging depth [48,49]. In PAI, a nanosecond pulsed laser is used to stimulate the biological sample wherein molecules absorb light energy

Figure 1. Overview of articular cartilage (AC) structure, composition, and function as acquired via optical tomography, vibrational spectroscopic, and elastography methods. (A) Graphical representation of the structure and biochemical composition of human articular cartilage. (B) Quantitative polarized light microscopy imaging of collagen fiber organization and orientation. Adapted, with permission, from [23]. (C) Hyperspectral Raman spectroscopy of AC composition and distribution, scale bar 50 μm. Adapted, with permission, from [24]. (D) OCE of AC with annotated (red arrow) subsurface defect, scale bar 500 μm. Adapted, with permission, from [25].

Table 1. Destructive and nondestructive modalities to evaluate structure, composition, and function of AC

	Traditional destructive assay		Alternative nondestructive assay			
	Modality	Measurand/attribute	Modality	Measurand	Refs	Example data
Structure	Histology	AC thickness	Polarized light microscopy	Refractive Index	[23]	Figure 1B
	Histology	Collagen fiber orientation	Polarized light microscopy	Birefringence w/polarization	[23,26]	Figure 1B Figure 2A
	Histology, Immunohistofluorescence	Collagen fiber orientation and architecture	Second-harmonic generation	Multiphoton interaction w/polarization	[27]	Figure 2B
	Histology, Immunohistochemistry	Tissue typing	Photoacoustic imaging	Photoacoustic	[28]	Figure 2C
	Histology/magnetic resonance imaging/X-ray	Extracellular matrix integrity and organization	Polarization sensitive optical coherence tomography	Birefringence w/polarization	[29]	
	Histology/magnetic resonance imaging/X-ray	AC thickness	Polarization sensitive optical coherence tomography	Refractive index	[30]	Figure 2D
Composition	Histology	Proteoglycan distribution	Fluorescence lifetime imaging	Endogenous fluorescence	[31]	Figure 3A
	Histology, immunohistochemistry, immunohistofluorescence	ECM composition and distribution	Raman spectroscopy/microspectroscopy	Inelastic light scattering (Raman scattering) of biomolecules	[24,32]	Figure 1C Figure 3C
	Histology	Proteoglycan distribution	Polarized light microscopy	Refractive index	[33]	Figure 3B
	Biochemical assay (Blyscan sulfated glycosaminoglycan assay)	Proteoglycan content	FT-IR	Biomolecular vibrational modes	[33]	Figure 3B
	Immunohistology, biochemical assay (Sircol Collagen Assay)	Collagen content and distribution	FT-IR	Biomolecular vibrational modes	[33]	Figure 3B
Function	Mechanical testing (e.g., uniaxial tension)	Stiffness	Ultrasound elastography	Bulk shear modulus	[34]	
	Mechanical testing (e.g., uniaxial tension)	Stiffness	Photoacoustic elastography	Bulk shear modulus	[35,36]	
	Mechanical testing (e.g., uniaxial tension)	Stiffness	OCE	Bulk shear modulus	[25,37,38]	Figure 1D Figure 5A–D

and convert it into heat (photoacoustic effect) resulting in a detectable rise in temperature. The thermoelastic expansion from the temperature rise generates acoustic waves which are detected by an ultrasonic transducer or a hydrophone. As sound scatters 1000 times less than light, the acoustic signal propagates much longer in biological tissue without significant attenuation [50]. This provides a nondestructive, real-time 3D imaging modality capable of evaluating changes in the tissue and detecting diseased states such as OA [51,52].

OCT is based on low-coherence interferometry, which measures the magnitude and echo time delay of backscattered light [53]. Lateral imaging resolution on the order of a few micrometers and imaging depth up to ~11 cm may be achieved. OCT systems can image cartilage tissue at micrometer (near-histological) resolution and millimeters in depth [54]. Real-time, fast 2D cross-sectional (Figure 2D) or 3D volumetric scans may also be achieved. Label-free, noninvasive, light-based interrogation of AC has been used to detect early signs of OA by imaging surface irregularities [54]. Additionally, polarization-sensitive OCT (PS-OCT) provides additional contrast and contains spatial information about the polarization state of light reflected from dis-organized pathological tissue [29]. Therefore, OCT/PS-OCT can produce analogous data to

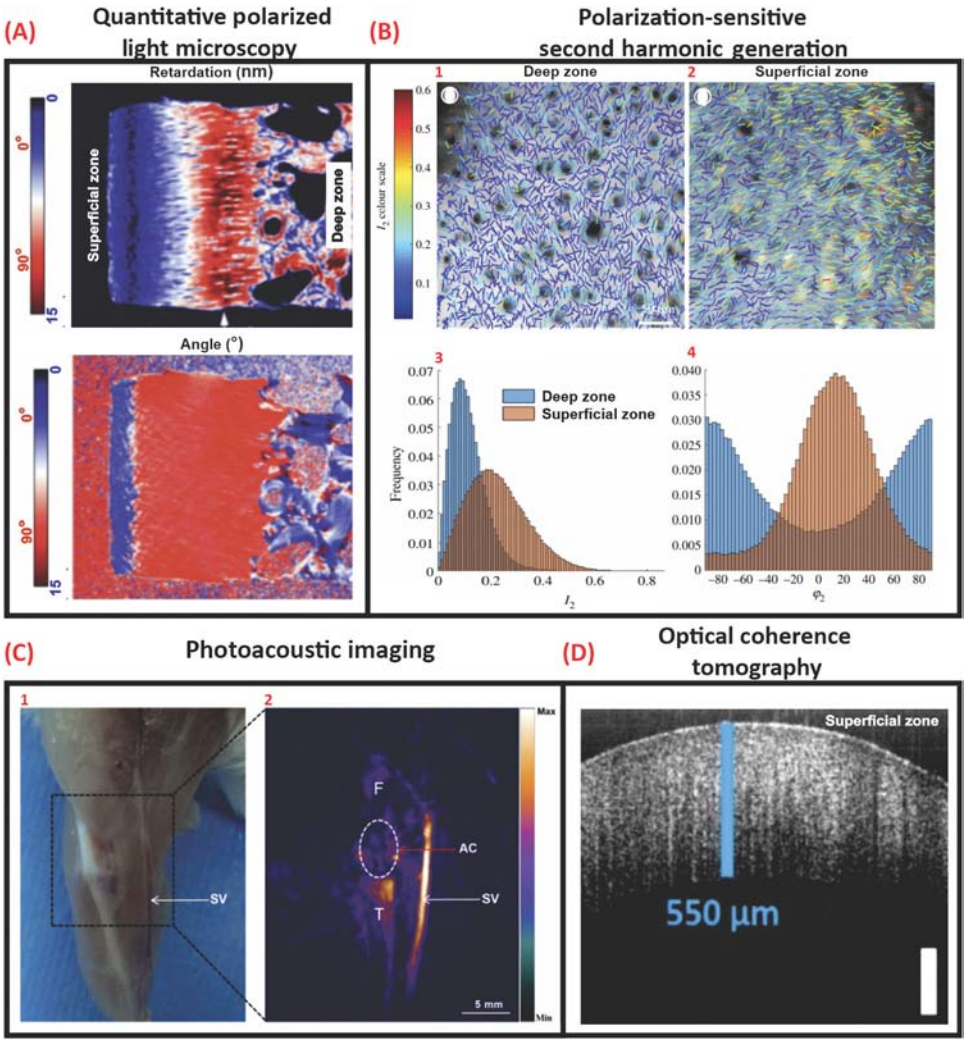

Figure 2. Optical interrogation of tissue structure. (A) Quantitative polarized light microscopy shows 2D retardation and angle images of the histological cartilage section. Adapted, with permission, from [24]. (B) Polarization-sensitive second-harmonic generation images illustrate a comparison between (1) deep zone and (2) superficial zone collagen organization in sections cut parallel with the articular surface in the same specimen. (3, 4) (I_2, φ_2) maps showing the collagen fiber orientations and degrees of isotropy. The direction of the lines represents collagen fiber alignment (φ_2) and the line color represents the degree of organization I_2 (higher I_2 representing more ordered collagen fibers). (3) The distribution of I_2 values over the superficial zone image and the deep zone image. (4) The distribution of φ_2 over the deep zone and superficial images (right), scale bar: 50 µm. Adapted, with permission, from [25]. (C) (1) Optical photograph, (2) Photoacoustic image of the right knee joint of a mouse. The region in the white circle is articular cartilage. Abbreviations: AC, articular cartilage; F, femur; SV, saphenous vein; T, tibia, scale bar: 5 mm. Adapted, with permission, from [26]. (D) OCT B scan of porcine anterior femoral head, scale bar: 250 µm. Adapted, with permission, from [28].

traditional histology as well as the capability of multiplanar optical sectioning allowing for volumetric examination of native and pathological tissue as well as TEMPs [39].

All three label-free and nondestructive imaging techniques are powerful tools and are suitable for *in vivo* imaging. Rapid, nondestructive testing methods with real-time feedback capabilities are clinically relevant; OCT and PAI probes are actively being designed and packaged for use with

existing arthroscopic tools [11,55,56]. The form factor of a probe is advantageous because only the probe needs to be sterilized. Probes can be incorporated with hand-held devices to address imaging needs during minimally invasive medical procedures such as endoscopy, tumor ablation, and intravascular imaging [30,57,58] as well as in-line biomanufacturing processes where aseptic direct interrogation of the sample is needed.

Optical interrogation of AC composition

AC ECM is a biochemically complex environment that directly affects its function. Histological and immunohistological tissue sections can be used to visualize and semiquantify the major components of AC ECM as well as temporally track tissue development [59]. Vibrational spectroscopy has been used to interrogate the biochemical composition of native and diseased tissue and validated by complementary histology (Figure 3B) to establish precedence for label-free analyses [33]. In addition to validating spectroscopic results, correlative spectroscopic and histological datasets provide reference data for the establishment and evolution of stand-alone vibrational spectroscopy-based nondestructive test methods to evaluate and characterize native and tissue-engineered AC [60].

Fluorescence lifetime imaging (FLIm) was evaluated as a nondestructive quantitative optical technique that can characterize tissues based on the endogenous autofluorescence of the primary tissue components (e.g., collagen and proteoglycans), as demonstrated in Figure 3A. FLIm utilizes the rate of exponential decay of endogenous fluorophores to generate maps of tissue biochemistry when excited by component-specific wavelengths. Through the acquisition and analysis of time-resolved fluorescence spectra via a fiber-coupled system, the detection of real-time biochemical changes in biological tissues *in vivo* and *in vitro* are achievable [61]. In a related study, the capacity of fiber-coupled FLIm as a potential diagnostic tool for the assessment of GAG-related OA was demonstrated by correlating GAG content and FLIm values [31]. This illustrates a current trend in spectral imaging wherein probes are deployable arthroscopically to evaluate zonal and depth-dependent structural and biochemical changes for diagnostic applications. Correlative diagnosis and tracking of disease progression by standard destructive assays to nondestructive methods typically serve as primary validators of new techniques leading to wider acceptance and adoption. Through this process, novel technologies, instruments, and methods can expand into other areas such as quality control and assurance in biomanufacturing workflows.

Brillouin microscopy is another spectral imaging technique that is based on Brillouin light scattering from acoustic waves or phonons in the GHz range for nondestructive contactless probing of the mechanics on a microscale [62]. Acoustic spectroscopy based on Brillouin scattering provides a detailed fingerprint of a material's micromechanics with microspectroscopic probes capable of high spatial (~1 μm) and spectral (~106 Hz) resolution [62]. Brillouin microscopy has been used to investigate the effect of trypsin digestion on *ex vivo* sections of porcine articular cartilage to verify the diagnostic capabilities of Brillouin microscopy as a detector of early OA. Small changes in water uptake were detected (>10× sensitivity when compared to quantitative magnetic resonance imaging) and were attributed to the loss of proteoglycan content. The authors purport these results as illustrative of the technique's capacity for early OA detection, as well as justification for pursuing further arthroscopic tool development by leveraging the accepted correlation between proteoglycan content and AC function. From a biomanufuacturing standpoint, a verified and validated assay based on this correlation may be suitable for temporal tracking of AC development by monitoring proteoglycan deposition and content. Not limited to AC, this and other techniques presented here should be critically evaluated for their suitability is assessing the critical quality parameters of a given TEMP.

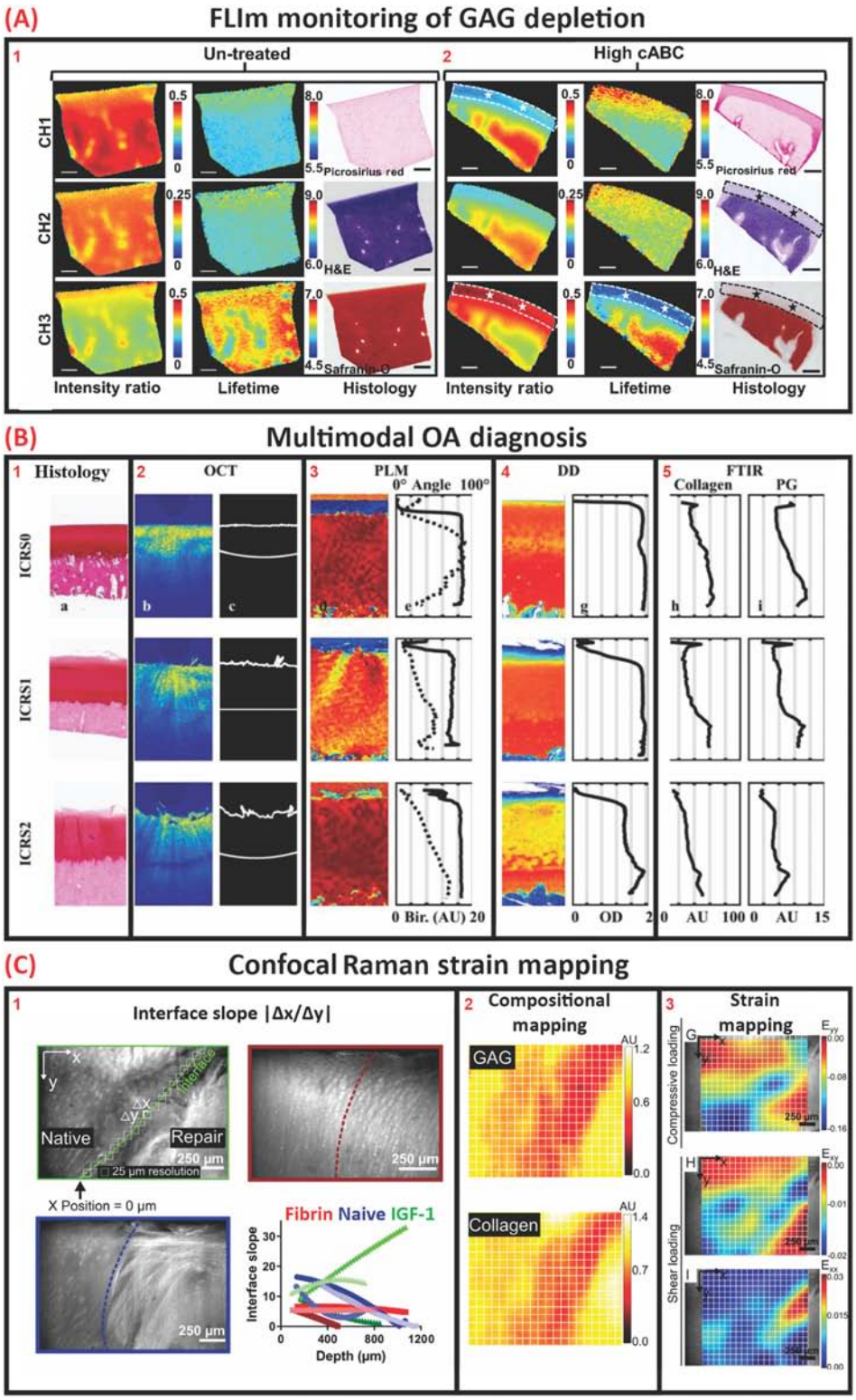

Trends in Biotechnology

(See figure legend at the bottom of the next page.)

Spectroscopic quantitation of AC composition

Near-infrared (NIR) spectroscopy is a nondestructive, real-time, and rapid vibrational spectroscopic technique used to characterize the state and composition of biological tissue. NIR spectroscopy operates between the 800- and 2500-nm region (4000–12 500 cm^{-1}) of the electromagnetic spectrum and is sensitive to molecular species containing C–H, N–H, O–H, and S–H, bonds found in the fundamental structures of biological materials [63]. Human tissues are transparent to light in the NIR spectral window and NIR light is either absorbed by pigmented compounds or scattered in tissues [64]. NIR spectroscopy nondestructively detects tissue oxygenation and enables *in vivo* evaluation of soft tissues due to its ability to penetrate deep into soft tissues. This capability may also be suitable for use in large volume bioreactors and cell culture using biologically inert and stable oxygen responsive compounds (e.g., iridium complexes) that emit detectable fluorescent and phosphorescent signals in free space for bulk measurements [65]. In addition, they may also be coupled to, or adsorbed upon, optical fibers/probes for point measurements or as embedded sensors in culture dishes/flasks.

Changes in AC structural properties as measured by OCT can be correlated to pathological changes in composition by **Fourier-transform infrared spectroscopy** (FT-IR), which operates in the mid-IR range of the electromagnetic spectrum between 5000 and 15 000 nm (400–4000 cm^{-1}). Recently, FT-IR has been used to compare and correlate histological sections of varying stages of tissue degeneration to nondestructive data of structure (OCT and PLM) and composition [**digital densitometry** (DD) and FT-IR] as shown in Figure 3B [33]. The study concluded that the system and methodology presented serves as a good model for detecting early-stage OA (i.e., Osteoarthritis Research Society International score 1–4). Depth-wise changes in proteoglycan content and collagen fiber structure on mechanical properties as a result of OA have been investigated [66,67]. By verifying and validating NIR and FT-IR coupled nondestructive assays and methodologies, a greater understanding of structure–function relationships has been obtained. Although NIR and FT-IR spectroscopy have shown potential, they are limited in their clinical utility due to the lack of minimally invasive tooling and instrumentation.

Another promising vibrational spectroscopy technique is **Raman spectroscopy**. This technique is based on inelastic light scattering (the Raman effect), which occurs when photons induce a change in the polarizability of molecules producing an optical fingerprint of the biomolecular constituents [68]. The intensity of the measured Raman spectra is linearly proportional to the concentration of molecular constituents [69]. Therefore, Raman spectroscopy is a noninvasive, label-free technique allowing for qualitative and semiquantitative analysis of AC ECM content and distribution at the molecular level [69]. Based on this specificity, Raman spectroscopy has been extensively used for quality control and assurance in industrial manufacturing; namely chemical/plastics manufacturing and semiconductors. Few examples of the use of Raman spectroscopy in the biomanufacturing of TEMPs have been reported [70,71].

Figure 3. Noninvasive modalities for biochemical interrogation for structural assessment and structural correlation. (A) Cross-sectional fluorescent lifetime image and corresponding histology section illustrating GAG distribution within bovine articular cartilage (untreated) and chrondroitinase–ABC-treated tissue with highlighted GAG-depleted regions, scale bar = 1 mm. Adapted, with permission, from [29]. (B) Exemplary images of ICRS0–2 scoring, which is indicative of severity of OA, as assessed by histology, OCT, PLM, and corresponding depth-dependent FTIR spectra for comparison and correlation. Adapted, with permission, from [32]. (C) (1) Optical images of the native-repair tissue interface and (2) corresponding hyperspectral confocal Raman map of GAG and collagen distribution. (3) Correlative heat map illustrating stress distribution under compressive and shear loading. Adapted, with permission, from [31]. Abbreviations: FTIR, Fourier-transform infrared spectroscopy; OA, osteoarthritis; OCT, optical coherence tomography.

Raman microscopes are typically built upon existing confocal microscope platforms which limits their access and applicability for in-line and in-process monitoring of biomanufacturing processes. To address this limitation, fiber-coupled Raman microspectrometers have been developed and are commercially available for various applications. Raman microspectroscopy has been used to track cell aggregate differentiation and ECM deposition [72]. In addition, Raman microspectroscopy has shown great promise for pathological diagnoses (spectropathology) and may be a strong candidate for bioprocess verification and validation [70,73]. Raman microspectrometers and other fiber-based spectroscopic techniques have begun to address multimodal integration by developing tools in a form-factor more amenable to coupling with other technologies to holistically assess native tissues and TEMPs. Through new probe development, miniaturization, and signal coupling and decoupling, structural, compositional, and functional information can be obtained through a single tool. In the following section, elastography and elastography-coupled techniques, which intend to correlate functional variances with changes in structure and composition, will be discussed.

Elastography testing of AC function

Tissue mechanics and mechanical properties have been widely used as surrogate measures of native tissue health, TEMP robustness, and projected TEMP clinical efficacy. Mechanically stressing and recording the tissue's response is standard clinical practice wherein a clinician palpates an area and registers the haptic response (typically stiffness and, conversely, elasticity) to locate symptomatic pain and abnormal growths or defects to render a diagnosis. Standardization of this practice evolved through the development, verification/validation, and clinical adoption of imaging modalities (e.g., ultrasound), wherein quantitative measures of these otherwise subjective analyses are made. Next, the imaging modalities which aim to add quantifiable values to the images of tissue deformation are discussed.

Elastography is the general term used to describe the use of biomedical imaging modalities to track and map the biomechanical properties of soft tissues (Figure 4). It involves three similar steps to manual palpation: mechanical or acoustic stimulation of the tissue, detection of said stimulation, and estimation of tissue elasticity. Ultrasound elastography is an early example of an elastography-coupled imaging modality to quantify tissue stiffness producing reliable, reproducible, and relevant clinical information. Not only limited to small areas or point measurements, areal mapping of tissue stiffness can be collected by capturing the strain field in the tissue under direct or indirect stress as shown in Figure 4A, or by the imaging of shear waves whose propagation is governed by the tissue stiffness rather than by its bulk modulus [74–76].

Photoacoustic elastography (PAE) is one example of nondestructive elastography-coupled imaging which quantitatively measures tissue stiffness and elasticity based on PAI. PAE uses a high-energy focused light source coupled to a tightly focused ultrasound transducer to capture pressure differences induced by quick (nanoseconds) illumination of a region of interest. It has shown promise in the research setting owing to its good spatial resolution (~60 μm) and penetration depth (in centimeters), allowing for noninvasive imaging of soft structures. Therefore, PAE has been limited to use in soft tissues and viscous fluids like vessels and blood [35], but not for stiffer tissues such as cartilage and bone. Recently, Jo and associates illustrated the feasibility of using fiber coupled PAI for OA prognosis by evaluating joint inflammation. The team expanded upon this work by developing a multifiber array allowing for multiplanar and volumetric analysis of hemoglobin oxygenation as an early-stage marker for OA [36]. Although work is active in PAE-based tissue characterization, to the authors' knowledge, no published studies have used this technique to AC. Because of the challenges of applying light-induced strain to stiff tissues such as cartilage, the application of direct and indirect mechanical stimulation coupled with optical

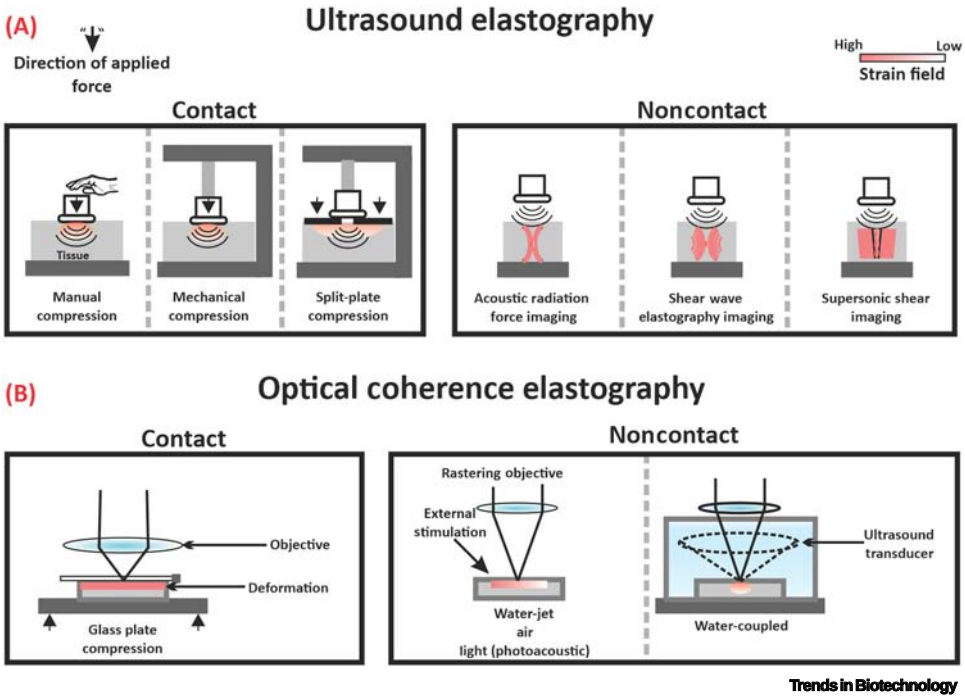

Figure 4. Overview of elastography and elastography-coupled technologies for single-cell and whole tissue characterization. This figure shows a schematic representation of (A) ultrasound elastography and (B) optical coherence elastography with exemplary images of contact and contactless stimulation used to interrogate tissue stiffness.

imaging (e.g., OCE) may have the potential of extending the applicability of elastography to the evaluation of stiff tissues.

OCE is a technique that incorporates elasticity measurements to polarized or nonpolarized OCT imaging. Contact and contactless methods of mechanical stimulation have been used to interrogate structure–function relationships as shown in Figure 4B. For example, Ravanfar and associates evaluated the effects of compression on collagen fiber orientation by polarization-sensitive OCT **tractography** and elastography, revealing a load-dependent response on radial zone fiber orientation as well as purporting the presence of discrete upper and lower radial zones. In addition, they derived a linear correlation between Δn and the logarithm of Young's modulus, which may serve as precedence for the establishment of an optical property-based functional measurement [77,78]. In another example of contact-based elastography, Wang and associates developed a water jet indentation biomicroscope for OA progression tracking [79]. Changes in mechanical properties due to tissue degeneration, as assessed by water jet indentation, correlated well with traditional destructive testing, prompting the authors to pursue packaging the components within existing arthroscopic tooling. Valid critiques of contact-based measurements include sample degradation due to the probe/stimulant as well as the inability to decouple noise from the actual signal. To address these concerns, contactless methods of mechanical stimulation have been investigated.

Multimodal testing of AC structure, composition, and function

Urban and associates used ARF to measure the shear modulus of tissue-engineered constructs by inducing and tracking shear wave vibrations in thin tissue constructs and tissue phantoms. The experimental results were compared to finite element models and numerical simulations, demonstrating concordance, and illustrating the potential of ARF-OCE [80]. Although good

corroboration was observed, limitations persist with ARF-OCE testing and its correlation to Young's modulus. This is primarily due to the anisotropic nature of most biological tissues and the unidirectionality of elastography measurements. To address this, Zhu and associates developed a biaxial method in which in-line and orthogonal shear waves can be captured relative to the OCT beam and combined to provide more appropriate and comparable elastography measurements [25]. Therefore, acoustically stimulated elastography tools may be suitable for analysis of inherently anisotropic tissues yielding relevant data including Young's modulus, Poisson's ratio, and shear modulus.

Recently, Hepburn and associates illustrated the capabilities of **OCT-coupled quantitative microelastography** (OCT-QME) to measure and correlate stress distribution as a factor of gel stiffness on single (Figure 5A) and multiple (Figure 5B) cells embedded within a bioactive hydrogel [37]. Through this work, they intend to understand the effects of microstrain on cell behavior which may be beneficial for in-process monitoring of developing tissues where mechanical stimulation may expedite tissue formation as well as produce morphologically similar and mechanically robust TEMPs. In another study, Fang and associates demonstrated the use of a handheld biaxial version of a modified commercially available OCT system with integrated quantitative microelastography for soft tissue strain mapping of breast tissue for cancer cell localization and cancer detection [38]. From an industrial perspective, the studies illustrate colocalized measurements of multiple parameters which may enable the reduction of testing equipment a facility would require to monitor the mechanical properties of TEMPs during biomanufacturing in a contactless manner.

Although OCT-based imaging has been clinically used to diagnose soft tissue diseases like macular degeneration, elastography-coupled OCT systems have yet to be implemented clinically, which may be due to the lack of understanding between changes in tissue optical properties and composition as well as function. In addition, current commercial systems are designed to interrogate open-air accessible tissues, limiting their clinical utility. However, like the fiber coupled nondestructive testing techniques previously described, miniaturization and packaging/retrofitting of existing tooling is currently being investigated to further the development and utility of multimodal fiber coupled nondestructive testing systems.

Concluding remarks and future perspectives

As active contributors toward the development and clinical translation of TEMPs for AC, we are cognizant of the steep and convoluted bench-to-bedside pathway for TEMP development and adoption. One of the initial steps when pursuing TEMP translation is a solid understanding of the end-use application and the underlying biological processes involved in TEMP development. With the advent of data mining and big data analytics, biomanufacturers may leverage these techniques to extensively survey open-source data repositories as well as published literature for empirical data elucidating critical correlates relevant to their specific TEMP to aid in decision-making processes. Big data may also help in highlighting voids in the literature, thus guiding basic research efforts as well as aid in harmonizing the field by establishing standardized language and data output.

Regulatory approval is another critical step towards TEMP development and successful clinical translation which is based on rigorous science-based testing by validated and standardized assays, protocols, and test methods to evaluate predefined critical quality attributes that can be correlated to measurable performance metrics. Regulatory guidelines for the approval of TEMPs are still evolving. Therefore, several outstanding questions persist and are highlighted (see Outstanding questions). Due to the relative nascency of the biomanufacturing industry, the

Outstanding Questions

Which critical measurands do biomanufacturers need to consider in order to deliver a useful, affordable, and valuable product to the clinic?

How can direct, nondestructive methods to assess critical quality components of TEMPs to monitor tissue maturation be best verified and validated?

How can we best standardize the language and data output to be better understood by multidisciplinary researchers and clinicians?

Can real-time feedback for in-process quality control benefit from artificial intelligence and machine learning to ensure/predict TEMP quality? How do we collect and collate the reference datasets necessary for algorithm development?

What resolution is the most suitable for clinical settings? Should device manufacturers stress high-resolution or high throughput?

How can we best standardize infrastructure requirements, as well as probe and sensor integration in biomanufacturing processes?

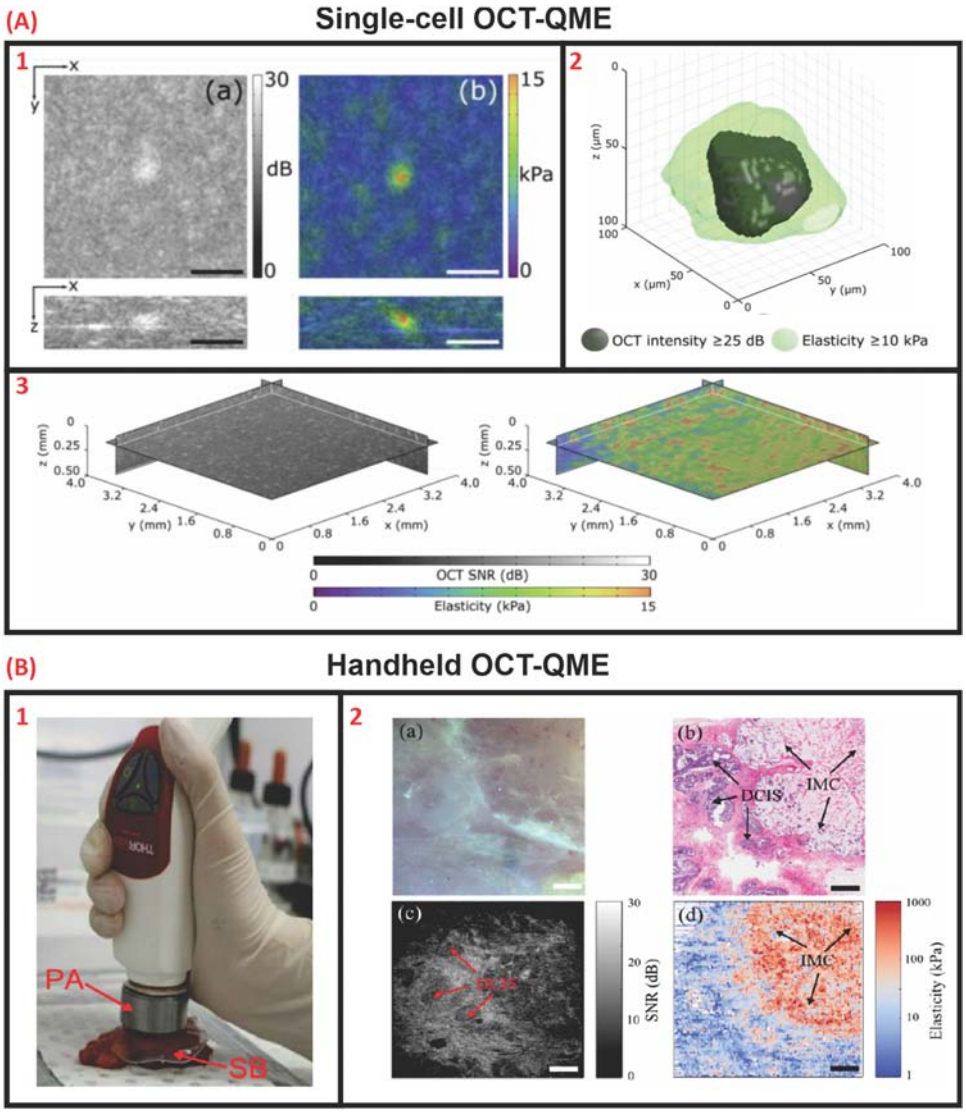

Trends in Biotechnology

Figure 5. Single-cell and handheld OCT-coupled quantitative microelastography. (A) (1) OCT-QME image and corresponding (2) 3D volumetric reconstruction of strain field of a single-cell embedded within a gelatin methacryloyl hydrogel, scale bar = 100 μm. (3) OCT-QME wide-field areal reconstruction of cell-embedded hydrogel [3.8 × 3.8 × 0.45 mm (x y z)]. Adapted, with permission, from [37]. (B) (1) An exemplary illustration of a handheld OCT-QME probe based on a commercially available OCT system for breast cancer diagnosis. (2) Optical, OCT, and histology imaging for verification and validation of the QME-generated elastogram, scale bar = 1 mm. Adapted, with permission, from [38]. Abbreviations: OCT, optical coherence tomography; OCT-QME, OCT-coupled quantitative microelastography.

burden of proof lies on the manufacturer to select and use suitable tests to produce adequate and appropriate results justifying the TEMPs indications for use. As with most burgeoning industries, the costs of manufacturing as well as the capital investment for test equipment become less prohibitive as the industry matures and validated technologies become more widely adopted.

Some of the nondestructive methods discussed here have the potential to be important tools for evaluating the intended structure, composition, and function of a TEMP, thus saving the

organization time and resources. Before implementation, well-designed and controlled studies directly correlating, for instance, linear attenuation (optical property) to glycosaminoglycan content (biochemical component) and its effect on shear modulus (mechanical property) are necessary. To that end, machine learning and artificial intelligence may prove beneficial when coupled to data mined or directly generated empirical data correlates. Machine learning/artificial intelligence-coupled nondestructive techniques may also overcome multiparametric issues related to aseptic in-line quality control and assurance monitoring by providing the capability of dynamically adjusting the biomanufacturing conditions thus increasing reproducibility and repeatability.

Therefore, there is a need for modernization of biomanufacturing processes (i.e., automation, protocol development and validation, and continuous nondestructive monitoring) to expedite the clinical translation of TEMPs as well as push the industry forward. We envision that the miniaturization/downsizing of the form factor of probes as well as the development of retrofitted and new single-/multimodal devices for minimally invasive assessment of tissues may prove suitable for deployment in in-process testing of TEMPs and for quality control and assurance in scalable bioprocesses.

Acknowledgments

Support for the work has been provided by an administrative supplement (PA-20-222) for R01 DE015058, as well as R01 AR071457 and R01 AR067821. G.B. acknowledges NIST National Research Council Post Doctoral Research Associateship. The authors gratefully acknowledge valuable discussions with Dr Irada Isayeva, Dr Jay Hoying, Dr Carl G. Simon, Dr Sumona Sarkar, Dr Nancy Lin, and Dr Sheng Lin-Gibson. These opinions, recommendations, findings, and conclusions do not necessarily reflect the views or policies of NIST or the United States Government.

Author contributions

N.J.C., G.B. wrote and J.H., K.A.A. edited the manuscript. All authors read and agreed to the published version of the manuscript.

Disclaimers

Official contribution of the National Institute of Standards and Technology; not subject to copyright in the United States. Certain commercial equipment, instruments, or materials are identified in this paper in order to specify the experimental procedure adequately. Such identification is not intended to imply recommendation or endorsement by the National Institute of Standards and Technology, nor is it intended to imply that the materials or equipment identified are necessarily the best available for the purpose.

Declaration of interests

The authors declare no competing financial interests.

References

1. ARMIIBioFabUSA, ed (2020) *BioFabUSA technical roadmap 2020 update*, ARMIIBioFabUSA. www.armiusa.org
2. Lee, M.H. *et al.* (2010) Considerations for tissue-engineered and regenerative medicine product development prior to clinical trials in the United States. *Tissue Eng. Part B Rev.* 16, 41–54
3. Hu, J.C. and Athanasiou, K.A. (2006) A self-assembling process in articular cartilage tissue engineering. *Tissue Eng.* 12, 969–979
4. Athanasiou, K.A. *et al.* (2013) Self-organization and the self-assembling process in tissue engineering. *Annu. Rev. Biomed. Eng.* 15, 115–136
5. Ofek, G. *et al.* (2008) Matrix development in self-assembly of articular cartilage. *PLoS One* 3, e2795
6. Cicchi, R. and Pavone, F.S. (2017) Probing collagen organization: practical guide for second-harmonic generation (SHG) imaging. *Methods Mol. Biol.* 1627, 409–425
7. Finnoy, A. *et al.* (2016) Second harmonic generation imaging reveals a distinct organization of collagen fibrils in locations associated with cartilage growth. *Connect. Tissue Res.* 57, 374–387
8. Moura, C.C. *et al.* (2019) Live-imaging of bioengineered cartilage tissue using multimodal non-linear molecular imaging. *Sci. Rep.* 9, 5561
9. Schenke-Layland, K. (2008) Non-invasive multiphoton imaging of extracellular matrix structures. *J. Biophotonics* 1, 451–462
10. McLean, J.P. *et al.* (2019) High-speed collagen fiber modeling and orientation quantification for optical coherence tomography imaging. *Opt. Express* 27, 14457–14471
11. Michalik, R. *et al.* (2019) Quantitative articular cartilage sub-surface defect assessment using optical coherence tomography: an *in-vitro* study. *Ann. Anat.* 221, 125–134
12. Pailhe, R. *et al.* (2018) Qualitative and quantitative assessment of cartilage degeneration using full-field optical coherence tomography *ex vivo*. *Osteoarthr. Cartil.* 26, 285–292
13. Reed, D.A. *et al.* (2019) Two-photon fluorescence and second harmonic generation characterization of extracellular matrix

remodeling in post-injury murine temporomandibular joint osteoarthritis. *PLoS One* 14, e0214072
14. Mahbub, S.B. *et al.* (2019) Non-invasive monitoring of functional state of articular cartilage tissue with label-free unsupervised hyperspectral imaging. *Sci. Rep.* 9, 4398
15. Li, Y. *et al.* (22 February 2019) Nondestructive method for chondrocyte viability assessment in articular cartilage tissues with nonlinear optical microscopy. In *Proc. SPIE 10882, Multiphoton Microscopy in the Biomedical Sciences XIX, 108822L*
16. Butler, H.J. *et al.* (2019) Shining a light on clinical spectroscopy: translation of diagnostic IR, 2D-IR and Raman spectroscopy towards the clinic. *Clin. Spectrosc.* 1, 100003
17. Querido, W. *et al.* (2017) Vibrational spectroscopy and imaging: applications for tissue engineering. *Analyst* 142, 4005–4017
18. Kumar, S. *et al.* (2016) Raman and infra-red microspectroscopy: towards quantitative evaluation for clinical research by ratiometric analysis. *Chem. Soc. Rev.* 45, 1879–1900
19. Kim, W. *et al.* (2016) Application of elastography for the noninvasive assessment of biomechanics in engineered biomaterials and tissues. *Ann. Biomed. Eng.* 44, 705–724
20. Mow, V.C. *et al.* (1992) Cartilage and diarthrodial joints as paradigms for hierarchical materials and structures. *Biomaterials* 13, 67–97
21. Gilbert, S.J. and Blain, E.J. (2018) Cartilage mechanobiology: how chondrocytes respond to mechanical load. In *In Mechanobiology in Health and Disease* (Verbruggen, S.W., ed.), pp. 99–126
22. Athanasiou, K.A. *et al.* (2019) *Articular Cartilage*, CRC Press
23. Rieppo, J. *et al.* (2009) Changes in spatial collagen content and collagen network architecture in porcine articular cartilage during growth and maturation. *Osteoarthr. Cartil.* 17, 448–455
24. Bergholt, M.S. *et al.* (2016) Raman spectroscopy reveals new insights into the zonal organization of native and tissue-engineered articular cartilage. *ACS Cent. Sci.* 2, 885–895
25. Zhu, J. *et al.* (2019) Acoustic radiation force optical coherence elastography for elasticity assessment of soft tissues. *Appl. Spectrosc. Rev.* 54, 457–481
26. Xia, Y. *et al.* (2001) Quantitative *in situ* correlation between microscopic MRI and polarized light microscopy studies of articular cartilage. *Osteoarthr. Cartil.* 9, 393–406
27. Mansfield, J.C. *et al.* (2019) Collagen reorganization in cartilage under strain probed by polarization sensitive second harmonic generation microscopy. *J. R. Soc. Interface* 16, 20180611
28. Chen, L. *et al.* (2018) Cationic poly-L-lysine-encapsulated melanin nanoparticles as efficient photoacoustic agents targeting to glycosaminoglycans for the early diagnosis of articular cartilage degeneration in osteoarthritis. *Nanoscale* 10, 13471–13484
29. de Boer, J.F. and Milner, T.E. (2002) Review of polarization sensitive optical coherence tomography and Stokes vector determination. *J. Biomed. Opt.* 7, 359–371
30. Jelly, E.T. *et al.* (2019) Optical coherence tomography through a rigid borescope applied to quantification of articular cartilage thickness in a porcine knee model. *Opt. Lett.* 44, 5590–5593
31. Zhou, X. *et al.* (2018) Detection of glycosaminoglycan loss in articular cartilage by fluorescence lifetime imaging. *J. Biomed. Opt.* 23, 1–8
32. Irwin, R.M. *et al.* (2021) Microscale strain mapping demonstrates the importance of interface slope in the mechanics of cartilage repair. *J. Biomech.* 114, 110159
33. Sarin, J.K. *et al.* (2017) Combination of optical coherence tomography and near infrared spectroscopy enhances determination of articular cartilage composition and structure. *Sci. Rep.* 7, 10586
34. Akkaya, M. *et al.* (2019) Sonoelastography of the knee joint. *Clin. Anat.* 32, 99–104
35. Schellenberg, M.W. and Hunt, H.K. (2018) Hand-held optoacoustic imaging: A review. *Photoacoustics* 11, 14–27
36. Jo, J. *et al.* (2018) Photoacoustic tomography for human musculoskeletal imaging and inflammatory arthritis detection. *Photoacoustics* 12, 82–89
37. Hepburn, M.S. *et al.* (2020) Three-dimensional imaging of cell and extracellular matrix elasticity using quantitative micro-elastography. *Biomed. Opt. Express* 11, 867–884
38. Fang, Q. *et al.* (2019) Handheld probe for quantitative micro-elastography. *Biomed. Opt. Express* 10, 4034–4049
39. Matcher, S.J. (2015) What can biophotonics tell us about the 3D microstructure of articular cartilage? *Quant. Imaging Med. Surg.* 5, 143–158
40. Keikhosravi, A. *et al.* (2017) Quantification of collagen organization in histopathology samples using liquid crystal based polarization microscopy. *Biomed. Opt. Express* 8, 4243–4256
41. Wang, K. *et al.* (2013) Depth-dependent refractive index of normal and early degenerated articular cartilage. *J. Biomed. Opt.* 18, 105003
42. Hyttinen, M.M. *et al.* (2001) Age matters: collagen birefringence of superficial articular cartilage is increased in young guinea-pigs but decreased in older animals after identical physiological type of joint loading. *Osteoarthr. Cartil.* 9, 694–701
43. Kiraly, K. *et al.* (1998) Articular cartilage collagen birefringence is altered concurrent with changes in proteoglycan synthesis during dynamic *in vitro* loading. *Anat. Rec.* 251, 28–36
44. Esquibel, C.R. *et al.* (2020) Second harmonic generation imaging of collagen in chronically implantable electrodes in brain tissue. *Front. Neurosci.* 14, 95
45. Chen, X.Y. *et al.* (2012) Second harmonic generation microscopy for quantitative analysis of collagen fibrillar structure. *Nat. Protoc.* 7, 654–669
46. Kumar, R. *et al.* (2015) Polarization second harmonic generation microscopy provides quantitative enhanced molecular specificity for tissue diagnostics. *J. Biophotonics* 8, 730–739
47. Bueno, J.M. *et al.* (2016) Second harmonic generation microscopy: a tool for quantitative analysis of tissues. In *Microscopy and Analysis* (Stanciu, S.G., ed.), IntechOpen
48. Hagiwara, Y. *et al.* (2015) Simultaneous evaluation of articular cartilage and subchondral bone from immobilized knee in rats by photoacoustic imaging system. *J. Orthop. Sci.* 20, 397–402
49. Liu, W.W. and Li, P.C. (2020) Photoacoustic imaging of cells in a three-dimensional microenvironment. *J. Biomed. Sci.* 27(1)
50. Attia, A.B.E. *et al.* (2019) A review of clinical photoacoustic imaging: current and future trends. *Photoacoustics* 16, 100144
51. Xiao, S. *et al.* (2020) Tracking osteoarthritis progress through cationic nanoprobe-enhanced photoacoustic imaging of cartilage. *Acta Biomater.* 109, 153–162
52. Guo, H. *et al.* (2019) Assessing the development and treatment of rheumatoid arthritis using multiparametric photoacoustic and ultrasound imaging. *J. Biophotonics* 12, e201900127
53. Drexler, W. and Fujimoto, J.G. (2015) *Optical Coherence Tomography : Technology and Applications*, Springer
54. Jahr, H. *et al.* (2015) Detecting early stage osteoarthritis by optical coherence tomography? *Biomarkers* 20, 590–596
55. Te Moller, N.C.R. *et al.* (2017) Semi-automated International Cartilage Repair Society scoring of equine articular cartilage lesions in optical coherence tomography images. *Equine Vet. J.* 49, 552–555
56. Puhakka, P.H. *et al.* (2016) Optical coherence tomography enables accurate measurement of equine cartilage thickness for determination of speed of sound. *Acta Orthop.* 87, 418–424
57. Lakin, B.A. *et al.* (2017) Assessing cartilage biomechanical properties: techniques for evaluating the functional performance of cartilage in health and disease. *Annu. Rev. Biomed. Eng.* 19, 27–55
58. Ansari, R. *et al.* (2018) All-optical forward-viewing photoacoustic probe for high-resolution 3D endoscopy. *Light Sci. Appl.* 7, 75
59. Decker, R.S. *et al.* (2015) Articular Cartilage: Structural and Developmental Intricacies and Questions. *Curr. Osteoporos. Rep.* 13, 407–414
60. Sarin, J.K. *et al.* (2019) Arthroscopic determination of cartilage proteoglycan content and collagen network structure with near-infrared spectroscopy. *Ann. Biomed. Eng.* 47, 1815–1826
61. Haudenschild, A.K. *et al.* (2018) Nondestructive fluorescence lifetime imaging and time-resolved fluorescence spectroscopy detect cartilage matrix depletion and correlate with mechanical properties. *Eur. Cell Mater.* 36, 30–43
62. Palombo, F. and Fioretto, D. (2019) Brillouin light scattering: applications in biomedical sciences. *Chem. Rev.* 119, 7833–7847
63. Afara, I.O. *et al.* (2018) Characterizing human subchondral bone properties using near-infrared (NIR) spectroscopy. *Sci. Rep.* 8, 9733
64. Curra, A. *et al.* (2019) Near-infrared spectroscopy as a tool for *in vivo* analysis of human muscles. *Sci. Rep.* 9, 8623

65. Kritchenkov, I.S. *et al.* (2021) Biocompatible Ir(III) complexes as oxygen sensors for phosphorescence lifetime imaging. *Molecules* 26, 2898
66. Saarakkala, S. *et al.* (2010) Depth-wise progression of osteoarthritis in human articular cartilage: investigation of composition, structure and biomechanics. *Osteoarthr. Cartil.* 18, 73–81
67. Ebrahimi, M. *et al.* (2020) Structure-function relationships of healthy and osteoarthritic human tibial cartilage: experimental and numerical investigation. *Ann. Biomed. Eng.* 48, 2887–2900
68. Bergholt, M.S. *et al.* (2019) Raman spectroscopy: guiding light for the extracellular matrix. *Front. Bioeng. Biotechnol.* 7, 303
69. Albro, M.B. *et al.* (2018) Raman spectroscopic imaging for quantification of depth-dependent and local heterogeneities in native and engineered cartilage. *NPJ Regen. Med.* 3, 3
70. Power, L. *et al.* (2019) Raman spectroscopy quality controls for GMP compliant manufacturing of tissue engineered cartilage. In *Proc. SPIE 10881, Imaging, Manipulation, and Analysis of Biomolecules, Cells, and Tissues XVII, 108810F*
71. Bergholt, M.S. *et al.* (2017) Online quantitative monitoring of live cell engineered cartilage growth using diffuse fiber-optic Raman spectroscopy. *Biomaterials* 140, 128–137
72. Kunstar, A. *et al.* (2011) Raman microspectroscopy: a noninvasive analysis tool for monitoring of collagen-containing extracellular matrix formation in a medium-throughput culture system. *Tissue Eng. Part C Methods* 17, 737–744
73. Hosu, C.D. *et al.* (2019) Raman spectroscopy applications in rheumatology. *Lasers Med. Sci.* 34, 827–834
74. McCredie, A.J. *et al.* (2009) Ultrasound elastography to determine the layered mechanical properties of articular cartilage and the importance of such structural characteristics under load. *Annu. Int. Conf. IEEE Eng. Med. Biol. Soc.* 2009, 4262–4265
75. Nieminen, H.J. *et al.* (2007) Ultrasound speed in articular cartilage under mechanical compression. *Ultrasound Med. Biol.* 33, 1755–1766
76. Ginat, D.T. *et al.* (2006) High-resolution ultrasound elastography of articular cartilage *in vitro*. *Conf. Proc. IEEE Eng. Med. Biol. Soc.* 6644–6647
77. Ravanfar, M. and Yao, G. (2019) Simultaneous tractography and elastography imaging of the zone-specific structural and mechanical responses in articular cartilage under compressive loading. *Biomed. Opt. Express* 10, 3241–3256
78. Ravanfar, M. and Yao, G. (2019) Measurement of biaxial optical birefringence in articular cartilage. *Appl. Opt.* 58, 2021–2027
79. Wang, Y. *et al.* (2014) An ultrasound biomicroscopic and water jet ultrasound indentation method for detecting the degenerative changes of articular cartilage in a rabbit model of progressive osteoarthritis. *Ultrasound Med. Biol.* 40, 1296–1306
80. Urban, M.W. *et al.* (2015) Characterization of material properties of soft solid thin layers with acoustic radiation force and wave propagation. *J. Acoust. Soc. Am.* 138, 2499–2507